OSSE Towards Quantifying ASCENDS Measurement Requirements to Constrain North American Regional CO_2 Fluxes

Janusz Eluszkiewicz, Marikate Mountain, Ryan Aschbrenner, John Henderson
Thomas Nehrkorn, Jennifer Hegarty, and Scott Zaccheo

Atmospheric and Environmental Research, Inc.

February 28, 2012

Overview of Regional Method

- Apply the **S**tochastic **T**ime-**I**nverted **L**agrangian **T**ransport (STILT) model driven by meteorological fields from the **W**eather **R**esearch and **F**orecasting (WRF) model to generate surface influence functions, "footprints", for ASCENDS observations.

- The "footprints" (or adjoint) express the sensitivity of ASCENDS column CO_2 observations to surface fluxes in the upwind source regions.

- Footprints enable the computation of posterior flux error reductions resulting from the inclusion of ASCENDS observations.

Atmospheric and Environmental Research

ASCENDS Candidate CO_2 Wavelengths

<u>3 Concepts:</u>

2.05µm [*Caron and Durand*, 2009]

1.57 µm

- 10pm offset
- 3 & 10pm offsets

2.05µm region has greatest sensitivity to near surface CO_2

BUT…

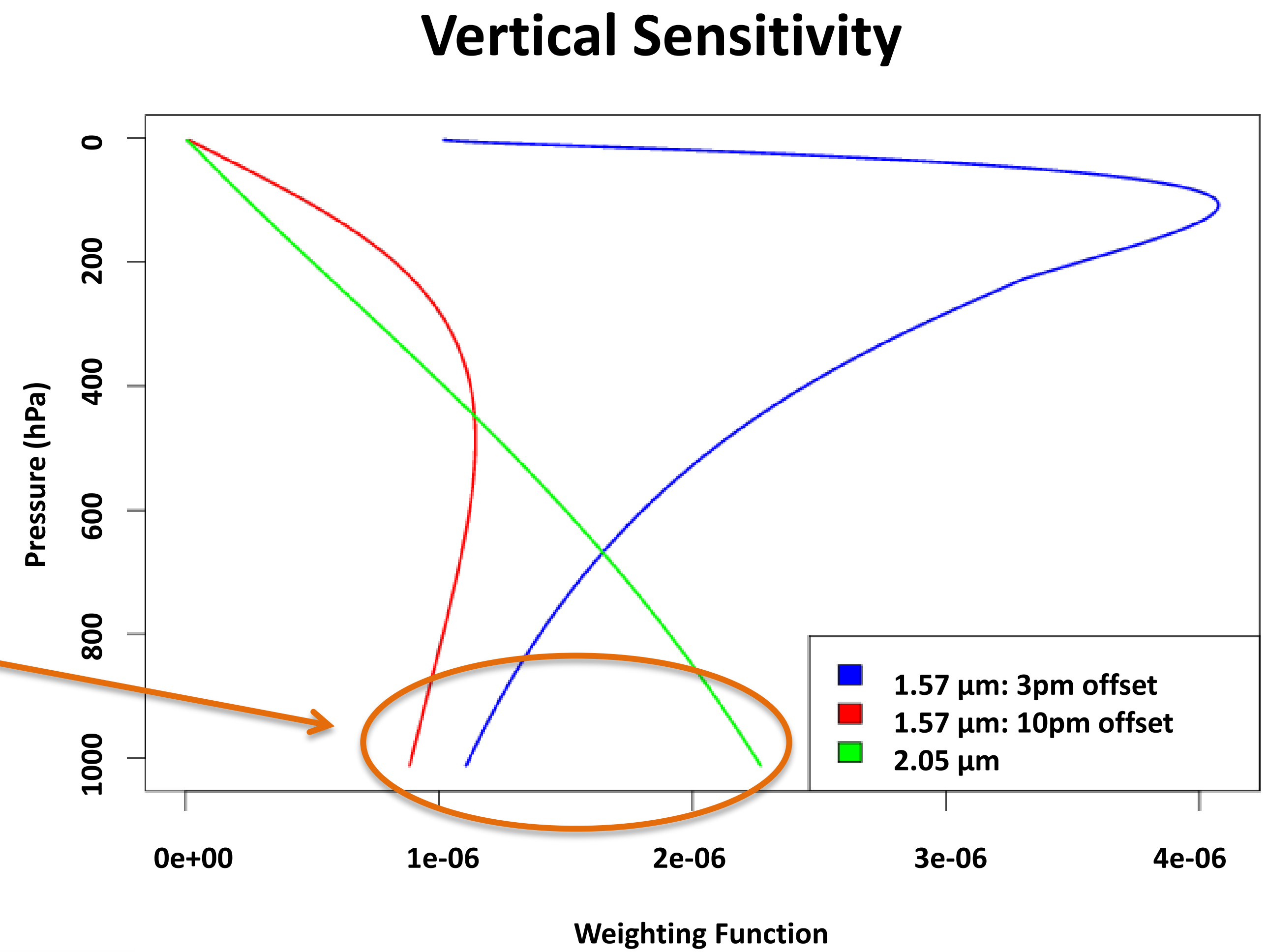

Atmospheric and Environmental Research

ASCENDS Candidate CO_2 Wavelengths

Measurement Errors for 1.57µm vs 2.05µm

2.05µm region has largest measurement errors

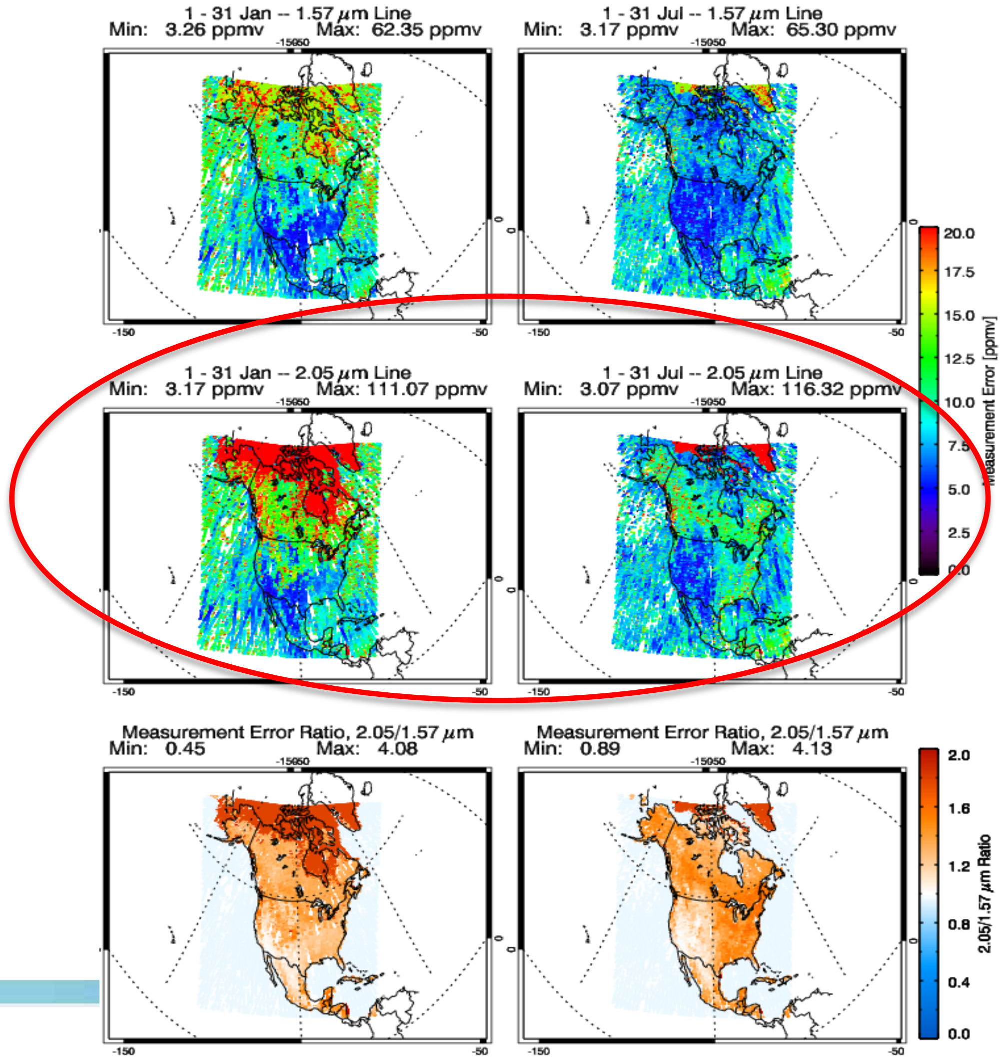

aer Atmospheric and Environmental Research

WRF-STILT

WRF [*Skamarock and Klemp*, 2008] :

•Mesoscale meteorological model provides transport fields

STILT [*Lin et al.*, 2003] :

•A Lagrangian (airmass-following) transport model allowing backward in time transport simulations (receptor-oriented).

•Minimizes numerical diffusion present in Eulerian models [*Chevallier et al.,* 2007].

•Efficient way to calculate adjoint ("footprint") at high spatial and temporal resolution.

WRF-STILT Coupling [*Nehrkorn et al.*, 2010] :

•Realistic treatment of convective fluxes.

•Good mass conservation properties.

WRF-STILT Application

Identify Receptor List

- Receptors – represent ASCENDS observation locations
- Receptor selection performed using CALIPSO orbital data over North America
  - Optical depth < 0.7
  - Surface detection frequency > 0
  - ~6,000 unique locations per day for Jan, Apr, Jul, and Oct 2007
  - Expand receptor list to 15 vertical levels (0.5 – 14.5km)

Trajectory Simulations

- WRF-STILT simulates release of 500 particles at each of the 15 levels for each receptor.
- Transport modeled backwards in time for 10 days.

aer Atmospheric and Environmental Research

WRF-STILT Application

STILT

- Revision 640 (www.stilt-model.org)

WRF Physics and Numerics

Option	Description
Land-surface	Noah land-surface model with Monin-Obukov surface layer
PBL package	Yongsei University (YSU) scheme
LW radiation	RRTM
SW radiation	Goddard
Microphysics	Lin et al.
Convection	Grell-Devenyi
Nudging	u,v,T,q at all levels above PBL, every 3 hours, 1 hour relaxation time
Time stepping	3rd order Runge-Kutta
Advection	5th order horizontal, 3rd order vertical positive definite advection for moisture and scalars
Diffusion	2nd order horizontal diffusion using Smagorinsky first-order closure
Damping	No upper level or vertical velocity damping; default values for divergence and external model damping

WRF

- Version 2.2
- 40km resolution
- NARR 32km grids for IC and BC
- 30 hr forecasts, reinitialized every 24 hrs with 6 hrs spin-up.
- Hourly output fields fed to STILT.

Atmospheric and Environmental Research

Footprint

•Quantitatively describes how much of total mixing ratio at a receptor comes from surface fluxes originating in upwind regions

•Generated by WRF-STILT

•Units: mixing ratio per unit flux $\left[\dfrac{ppmv}{\mu mol / m^2 / s}\right]$

•Domain: 11-65N, 50-170W

•Resolution: 1 deg horizontal & 3 hourly, 10 days back

•One unique location has 15 footprint maps – one for each vertical level

Vertically Integrated Footprint

•Quantitatively describes how much of column mixing ratio comes from surface fluxes originating in upwind regions.

•Convolve 15 levels of footprint maps for each receptor with lidar weighting functions.

Vertically Integrated Footprints

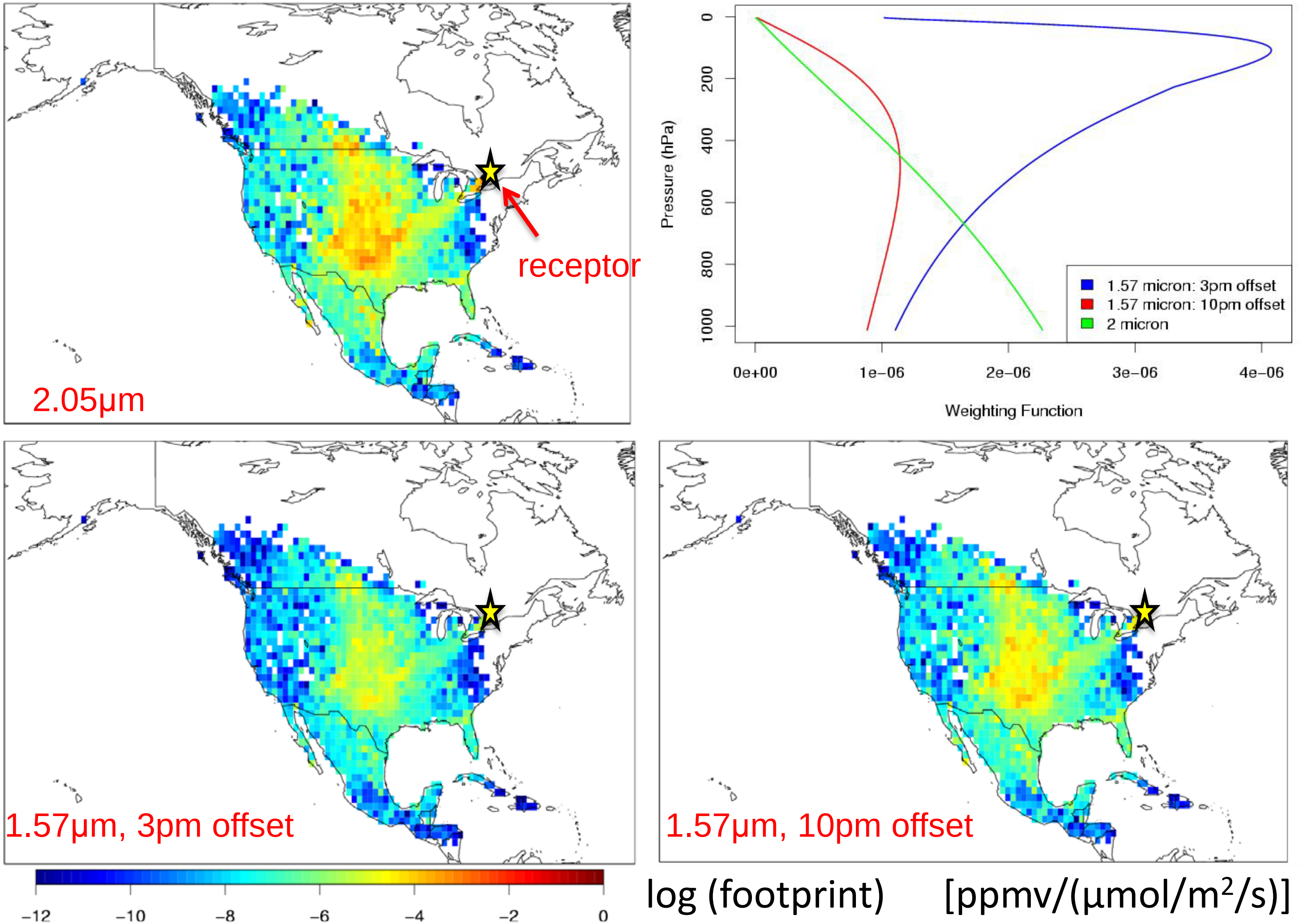

log (footprint) [ppmv/(μmol/m²/s)]

Atmospheric and Environmental Research

Formally Relate Footprint and Column CO_2

$$\Delta C(x_r, y_r, t_r) = \sum_{veg\ n=1}^{N} \int_{z_r=0}^{15km} w(z_r) \iiint_{x\,y\,t} f(x,y,t|x_r,y_r,t_r,z_r) * \varpi_n(x,y) * \left[F_n^{prior} + d_n\right] * dxdydtdz_r$$

$$+ \int_{z_r}^{15km} w(z_r) \iiint_{x\,y\,t} f(x,y,t|x_r,y_r,t_r,z_r) * F_{anthro}^{prior} * \alpha_{anthro} * dxdydtdz_r$$

Simplifies to

$$\Delta C(x_r, y_r, t_r) = \sum_{veg\ n=1}^{N} K_n(x_r, y_r, t_r) * \left[F_n^{prior} + d_n\right] + K_{anthro} * \alpha_{anthro}$$

GREEN = vegetative BLUE = anthropogenic

$\Delta C(x_r, y_r, t_r)$ =change in CO2 column mixing ratio at (x_r, y_r, t_r)

$f(x,y,t|x_r,y_r,t_r,z_r)$ = footprint matrix at (x_r,y_r,t_r,z_r)

$w(z_r)$ = 1 of 3 possible weighting functions

$\varpi_n(x,y)$ = vegetative coverage fraction at (x,y)

F_{anthro}^{prior} = a priori anthropogenic flux

F_n^{prior} = prior flux for vegetation type n

α_{anthro} = multiplicative anthropogenic flux factor

α_n = additive flux factor for vegetation type n

aer Atmospheric and Environmental Research

K_{anthro} & K_n

Anthropogenic (K_{anthro})

•Calculate using fluxes from the Vulcan Project anthropogenic emission inventory [*Gurney et al.*, 2009]

Vegetative (K_n)

•Calculate based on 11 vegetation types defined in in the Vegetation Photosynthesis and Respiration Model (VPRM) [*Mahadevan et al.*, 2008]

11 Vegetation Types Fraction Coverage

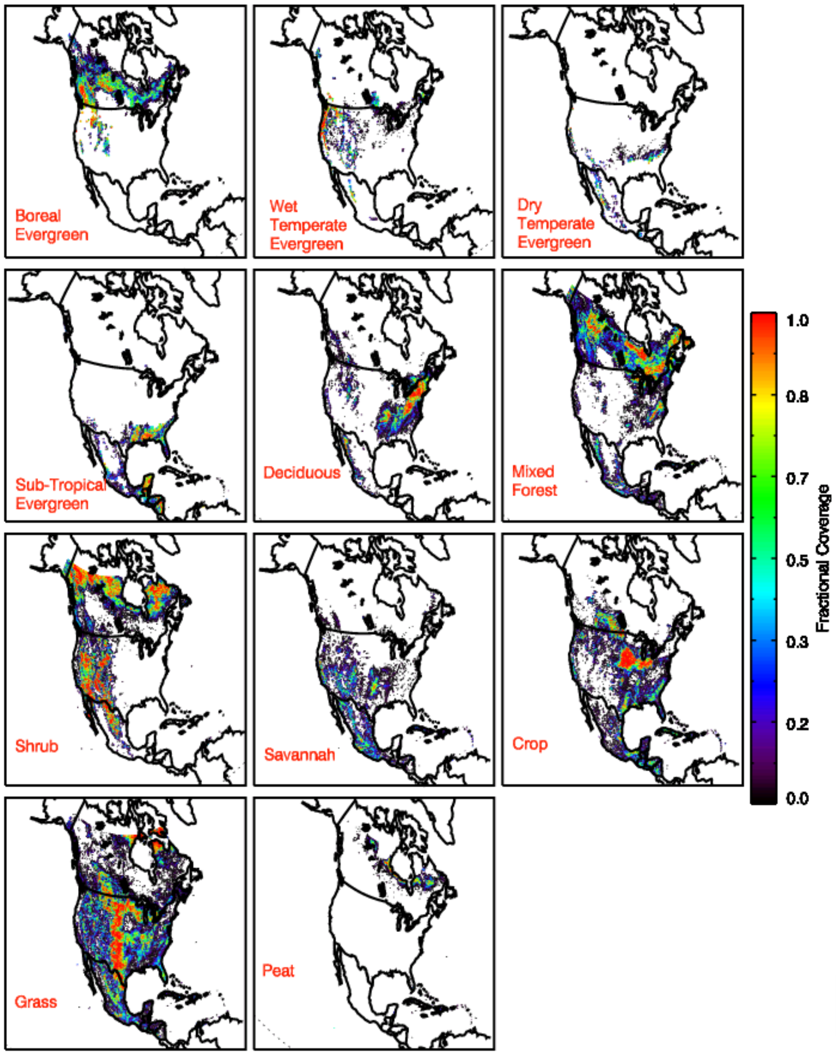

A Posteriori CO_2 Flux Error

Apply integrated footprints K_n and K_{anthro} to calculate *a posteriori* CO_2 flux error due to introduction of ASCENDS observations:

$$\hat{S}_{post} = \left(\hat{K}^T \hat{S}_{\varepsilon}^{-1} \hat{K} + \hat{S}_{prior}^{-1}\right)^{-1}$$

$$\hat{S}_{post} = \text{a posteriori flux errors } (\sigma_{post}^2)$$

$$\hat{K} = \text{vegetative } (K_n) \text{ or anthropogenic } (K_{anthro}) \text{ integrated footprint}$$

$$\hat{S}_{\varepsilon} = \text{measurement error matrix}$$

$$\hat{S}_{prior} = \text{a posteriori flux errors } (\sigma_{prior}^2)$$

Atmospheric and Environmental Research

A Priori Flux Errors

Vegetative

- Apply $\hat{S}_{prior}$ calculated by *Matross* [2006] to Jan & Jul 2007
  - Calculated for 11 vegetation types in VPRM
  - Off diagonal elements assumed 0
  - Diagonal elements estimated for summer 2004

Anthropogenic

- Assume monthly mean *a priori* fractional error = 0.5 (overly pessimistic for Vulcan?)

aer
Atmospheric and Environmental Research

Measurement Errors

•Best case scenario

- Consider contributions from random instrument measurement errors
- Exclude contributions from: atmospheric transport
  lateral boundary condition
  fossil fuel signal [*Gerbig et al*., 2003]

•Calculation

- Diagonal matrix computed using reference value at Railroad Valley, NV (RRV)

δX_i = measurement error at receptor
$r_s(i)$ = surface reflectivity at recptor
$\tau^2_{atm}(i)$ = atmospheric transmission at recptor

$$\delta X_i = \delta X_0 \left[\frac{r_s(i)}{r_s(0)} \frac{\tau^2_{atm}(i)}{\tau^2_{atm}(0)} \right]^{-1/2}$$

δX_0 = measurement error at RRV
$r_s(0)$ = surface reflectivity at RRV
$\tau^2_{atm}(0)$ = atmospheric transmission at RRV

- Surface reflectivity from MODIS backscatter
- Optical depth from CALIPSO data

Measurement Errors

January **July**

1.57µm

2.05µm

Ratio: 2.05µm/1.57µm

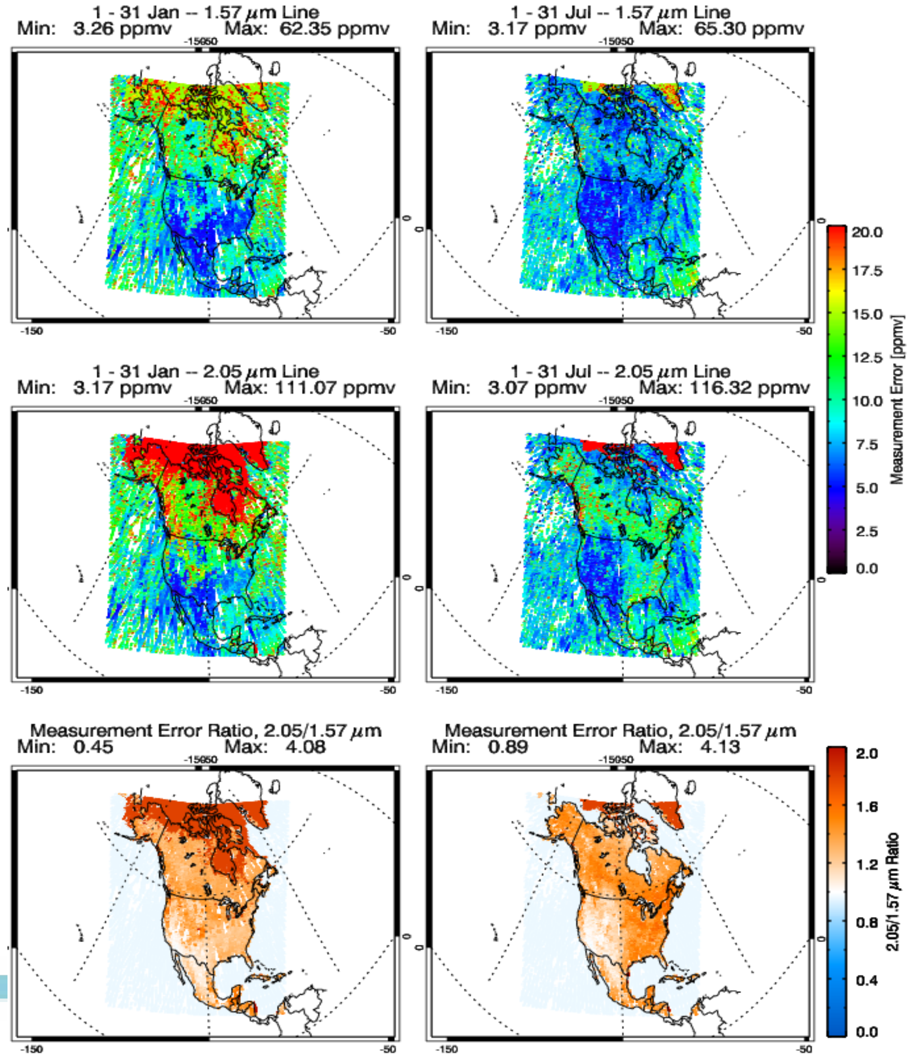

Atmospheric and Environmental Research

Baseline Results

1.) Types with large *a priori* have large posterior error reduction on small timescale

2.) Types with small fractional coverage have smaller reductions

3.) 3pm offset does little to improve upon 1.57μm at 10 pm offset

$$\text{posterior flux error reduction} = \left(1 - \frac{\sigma_{post}}{\sigma_{prior}}\right) * 100$$

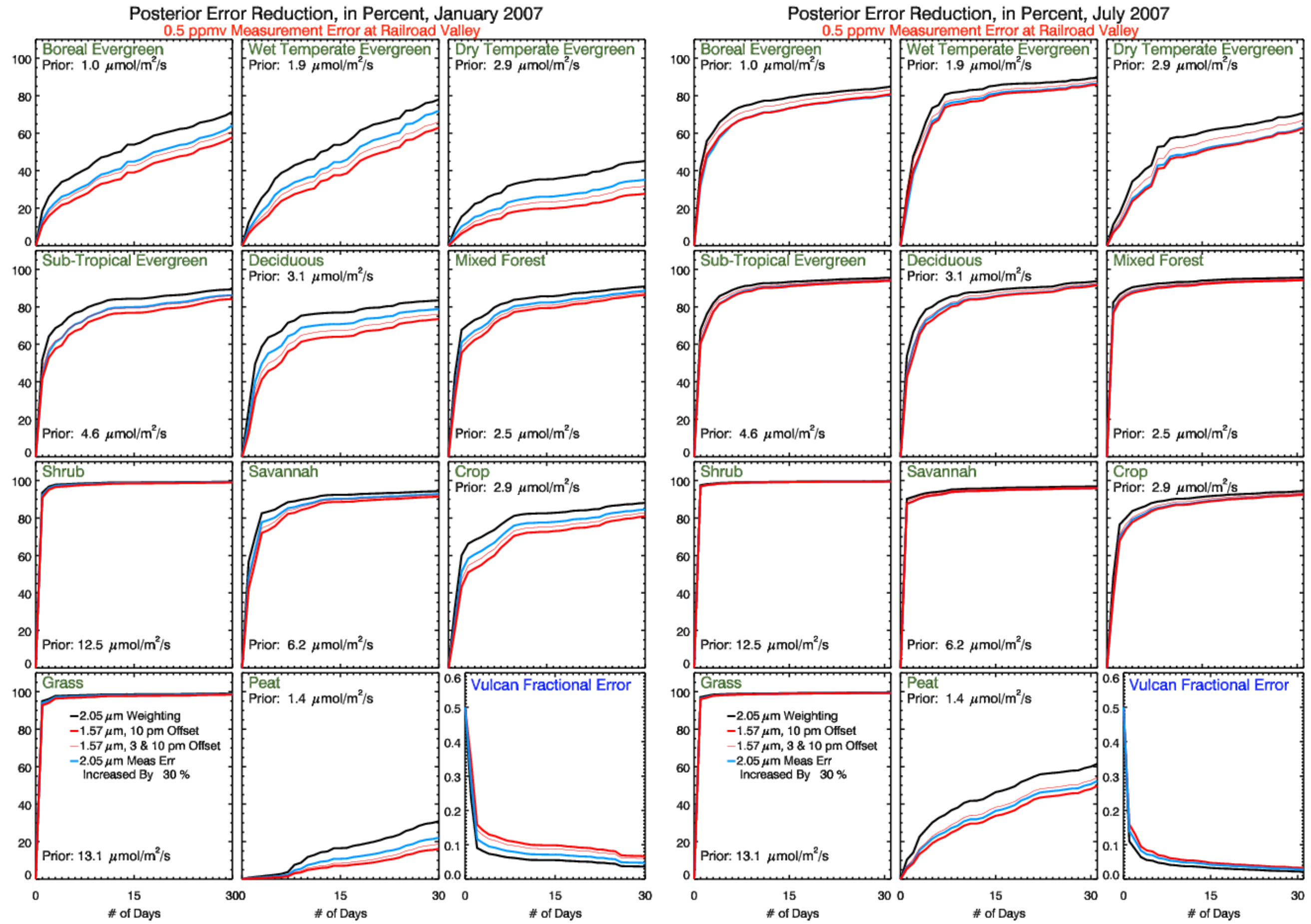

Baseline Results

4.) Greater flux error reductions for 2.05μm vs 1.57μm lines, particularly in January

5.) Modest increases in measurement error for 2.05μm line (blue) mask error reduction differences between lines

6) Flux error reductions are larger in July than January due to seasonality of measurement errors and regardless of weighting function

$$\text{posterior flux error reduction} = \left(1 - \frac{\sigma_{post}}{\sigma_{prior}}\right) * 100$$

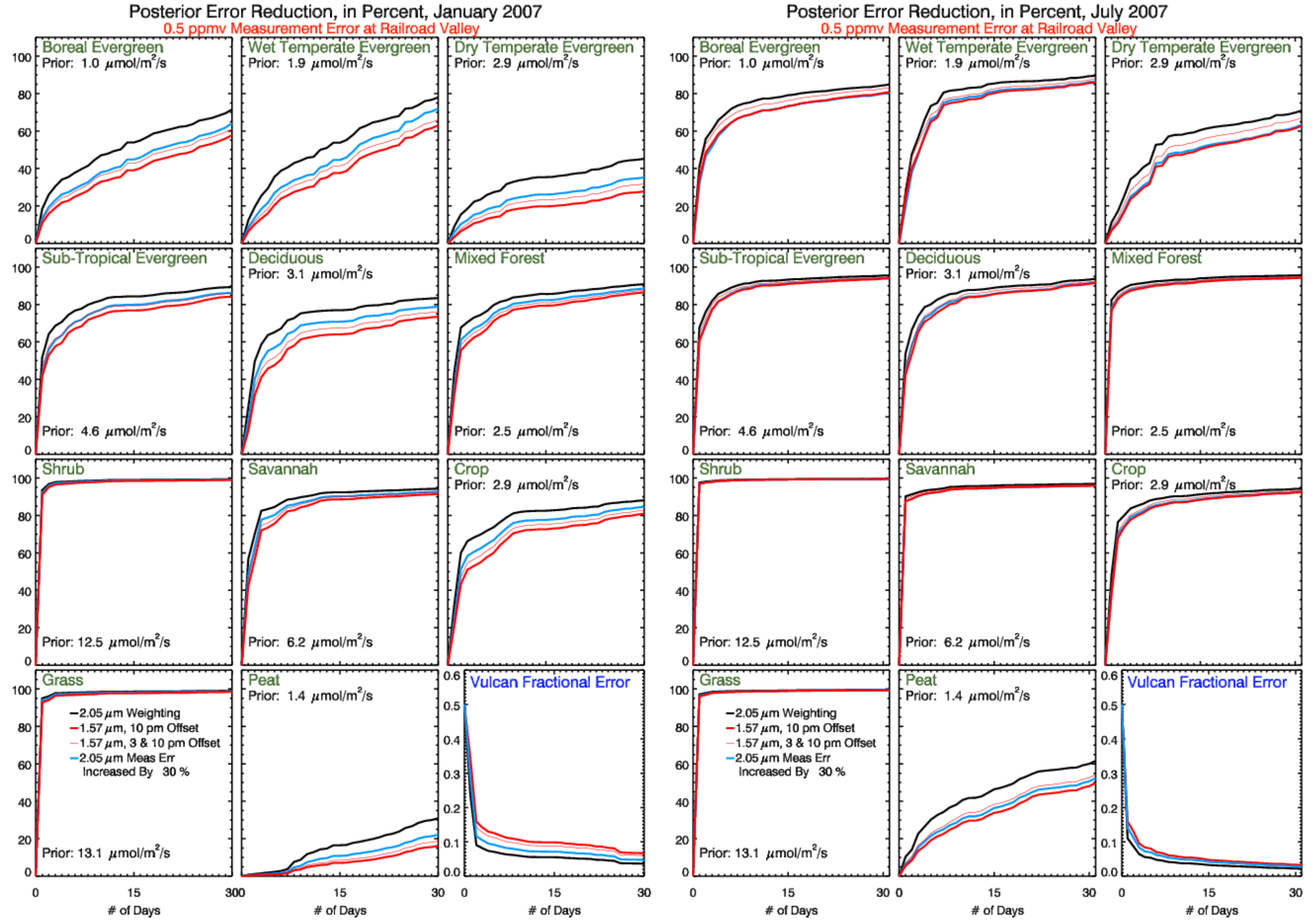

Results – Impact of Prior

1.) Most “prior-less” results converge with prior constraint counterparts

2.) Exceptions are those types with smaller fractional coverage.

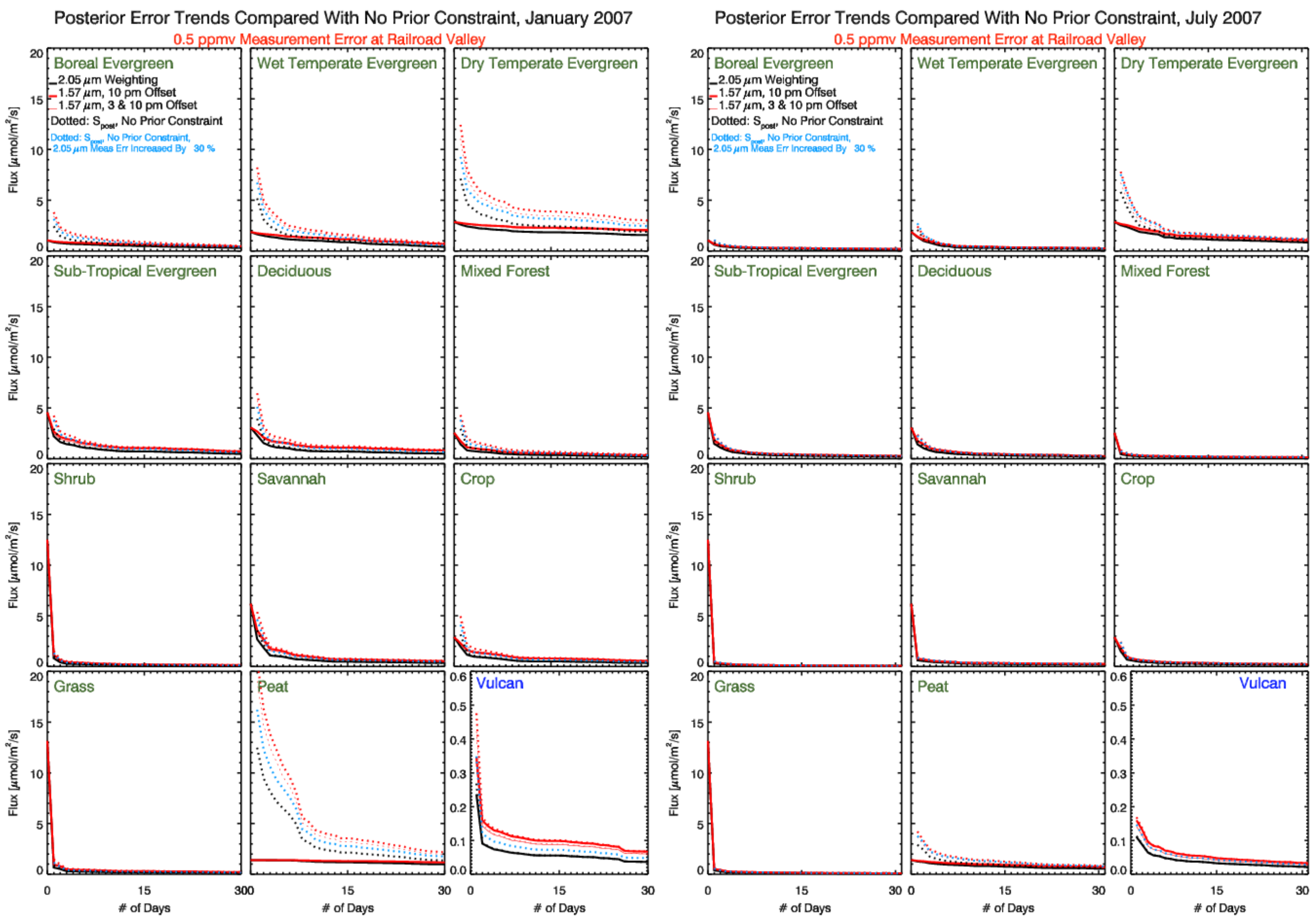

Results – Increasing Measurement Error At RRV

1.) Much smaller posterior error reductions as measurement error increased

0.5ppmv

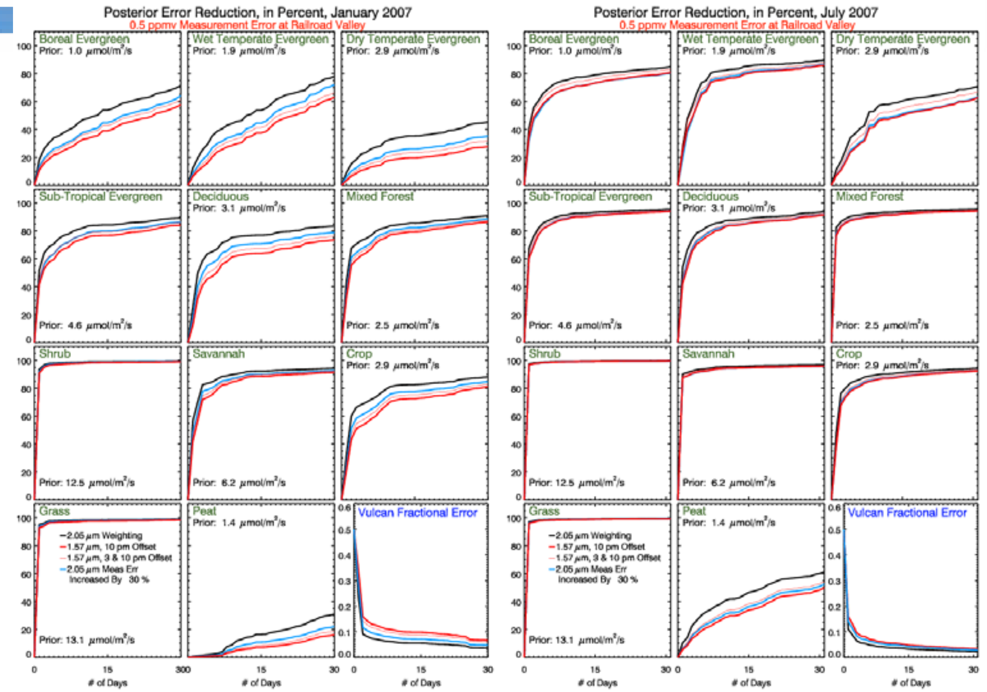

2) Larger posterior error reduction differences at 2.5ppmv

For larger measurement errors, up to ~1.5-3.5ppmv the advantage of a lower-peaking weighting function is more important to constraining fluxes

2.5ppmv

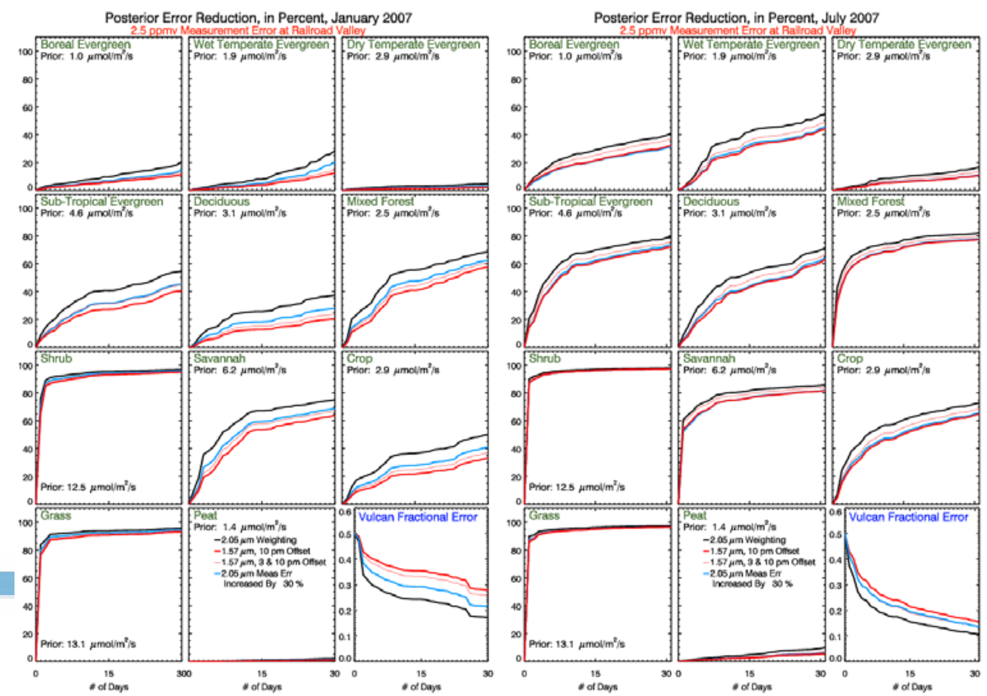

Results – Increasing Measurement Error At RRV

3.) As the measurement error increases, the prior constraint begins to dominate, particularly within the first 5 to 10 days, and impacting January more than July

0.5ppmv

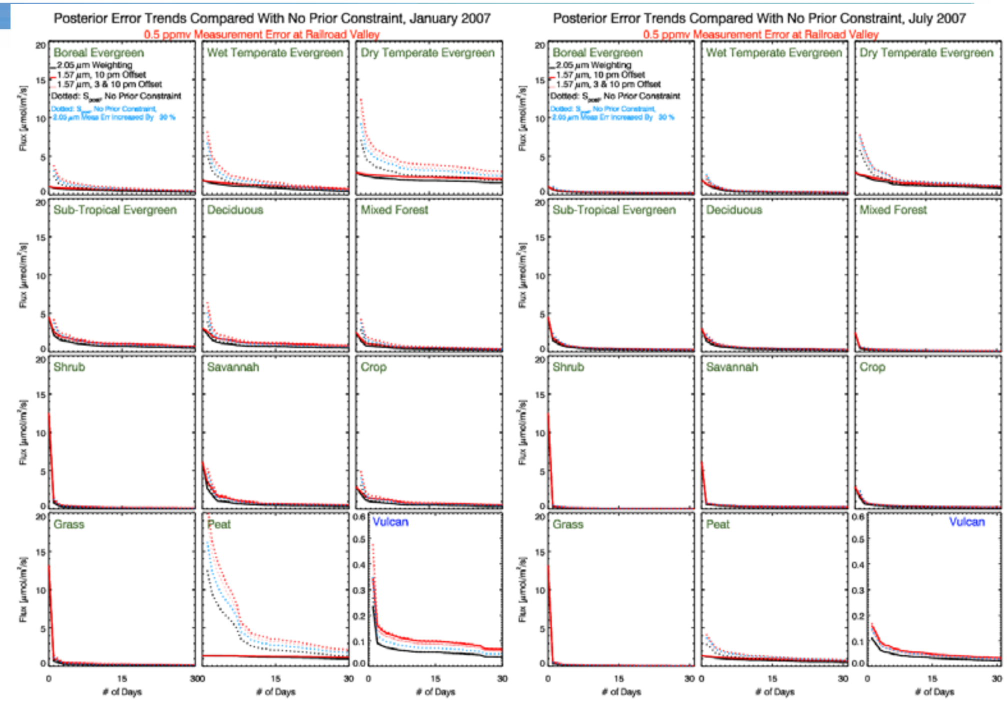

2.5ppmv

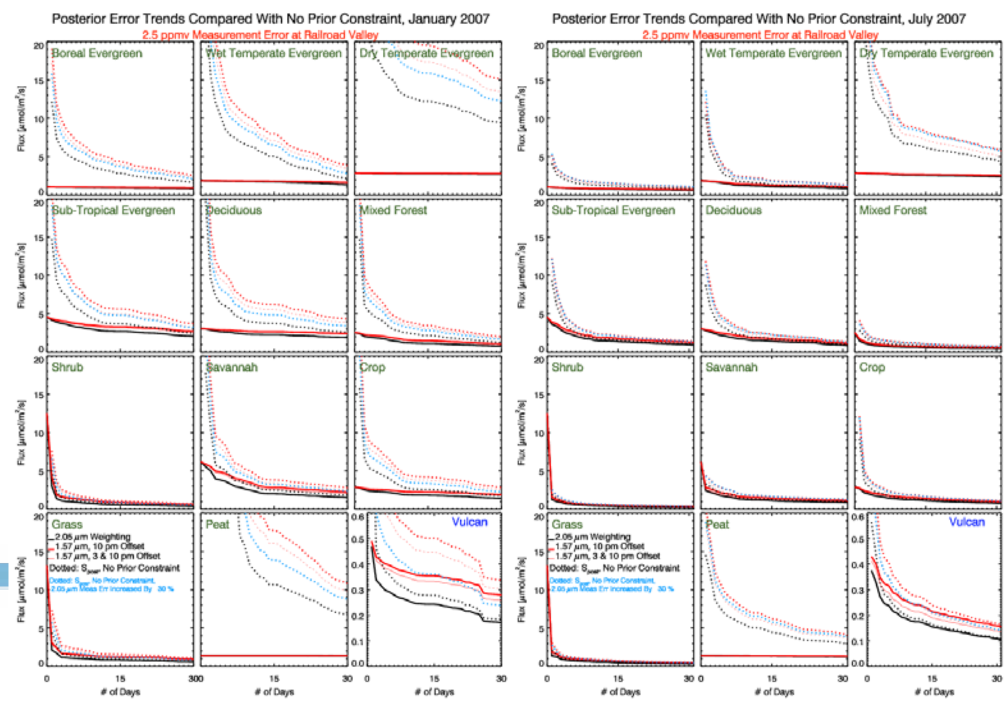

Atmospheric and Environmental Research

Results – Increasing Measurement Error at RRV

4) As expected, measurement error of 0.5ppmv achieves greatest posterior error reduction

5) Nonlinear behavior exhibited by most types except shrub and grass

Posterior Error Reduction After 1 Week

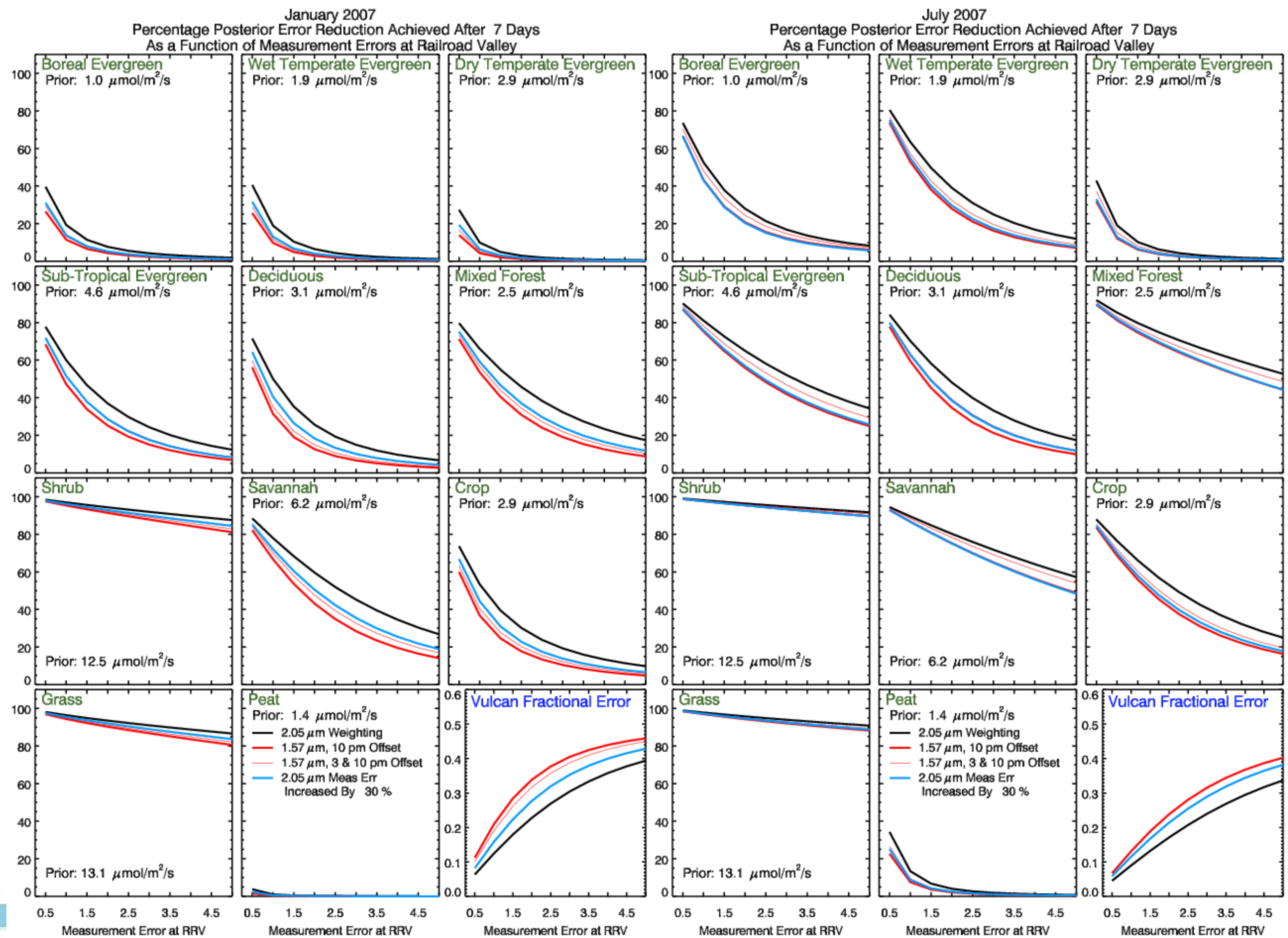

aer
Atmospheric and Environmental Research

Conclusions

Baseline

1.) Types with large *a priori* have large posterior error reduction on small timescale

2.) Types with small fractional coverage have smaller reductions

3.) 3pm offset does little to improve upon 1.57μm at 10 pm offset

4.) Greater flux error reductions for 2.05μm vs 1.57μm lines, particularly in January but modest increases in measurement error for 2.05μm line mask error reduction differences between lines

5.) Flux error reductions are larger in July than January due to seasonality of measurement errors and regardless of weighting function

Prior Constraint

6.) The prior constraint has a limited impact on results at measurement error of 0.5 ppmv at RRV

Measurement Error

7.) As measurement error increases, there is a nonlinear decrease in reduction of posterior error

8.)For larger measurement errors, up to ~1.5-3.5ppmv the advantage of a lower-peaking weighting function is more important to constraining fluxes

9.) As the measurement error increases, the prior constraint begins to dominate, particularly within the first 5 to 10 days, and impacting January more than July

aer
Atmospheric and Environmental Research

Future

•The footprint library provides valuable input to cost-benefit analyses of ground-based versus space-borne approaches to Measurement, Reporting, and Verification (MRV).

•The footprint library can be utilized in many other applications because footprint maps are not dependent on:

- •vertical weighting function or averaging kernel
- •measurement random errors
- •*a priori* flux errors
- •surface cover type and inversion approach
- •molecular species (i.e., footprints can be applied to gases other than CO_2).

•The footprint library underlying this study has been computed on a daily basis for January, April, July, and October 2007 and is available to researchers with access to Pleiades (please contact jel@aer.com for more information).

aer
Atmospheric and Environmental Research

Acknowledgements

- This work has been funded by the NASA Atmospheric CO_2 Observations from Space Program (grant NNX10AT87G).

- ASCENDS Measurement Requirement Definition team, especially
    - Randy Kawa
    - Ed Browell
    - Jim Abshire
    - Bob Menzies
    - Berrien Moore

- Dan Matross

- NASA Ames HEC facility staff

Atmospheric and Environmental Research

Thank You

References

Caron, J. and Y. Durand (2009), Operating wavelengths optimization for a spaceborne lidar measuring atmospheric CO_2, *Appl. Opt. 48,* 5413-5422.

Chevallier, F., F.-M. Bre on, and P. J. Rayner (2007), Contribution of the Orbiting Carbon Observatory to the estimation of CO_2 sources and sinks: Theoretical study in a variational data assimilation framework, *J. Geophys. Res., 112,* D09307, doi:10.1029/2006JD007375.

Gerbig, C., J. C. Lin, S. C. Wofsy, B. C. Daube, A. E. Andrews, B. B. Stephens, P. S. Bakwin, and C. A. Grainger (2003), Towards constraining regional scale fluxes of CO_2 with atmospheric observations over a continent: 2. Analysis of COBRA data using a receptor-oriented framework, *J. Geophys. Res., 108* (D24), 4757, doi:10.1029/2003JD003770.

Gurney, K.R., D.L. Mendoza, Y. Zhou, M.L. Fischer, C.C. Miller, S. Geethakumar, and S. de la Rue du Can (2009), High Resolution Fossil Fuel Combustion CO2 Emission Fluxes for the United States, *Environ. Sci. & Technol. 43* (14), 5535-5541, doi:10.1021/es900806c.

Kawa, S. R., D. J. Erickson III, S. Pawson, and Z. Zhu (2004), Global CO_2 transport simulations using meteorological data from the NASA data assimilation system, *J. Geophys. Res.*, 109, D18312, doi:10.1029/2004JD004554.

Lin, J. C., C. Gerbig, S. C. Wofsy, B. C. Daube, A. E. Andrews, K. J. Davis, and C. A. Grainger (2003), A near-field tool for simulating the upstream influence of atmospheric observations: The Stochastic Time-Inverted Lagrangian Transport (STILT) model, *J. Geophys. Res., 108(D16),* 4493, doi:10.1029/2002JD003161.

Mahadevan, P., S. C. Wofsy, D. M. Matross, X. Xiao, A. L. Dunn, J. C. Lin, C. Gerbig, J. W. Munger, V. Y. Chow, and E. W. Gottlieb (2008), A satellite-based biosphere parameterization for net ecosystem CO_2 exchange: Vegetation Photosynthesis and Respiration Model (VPRM), *Global Biogeochem. Cycles*, *22*, GB2005, doi:10.1029/2006GB002735.

Matross, D. M. (2006), Regional Scale Land-Atmosphere Carbon-Dioxide Exchange: Data Design and Inversion within a Receptor Oriented Modeling Framework, PhD Thesis, Department of Earth and Planetary Sciences, Harvard University, 171 pp.

Nehrkorn, T., J. Eluszkiewicz, S. C. Wofsy, J. C. Lin, C. Gerbig, M. Longo, and S. Freitas (2010), Coupled Weather Research and Forecasting/Stochastic Time-Inverted Lagrangian Transport (WRF-STILT) model, *Meteor. Atmos. Phys., 107 (1-2),* 51–64, doi:10.1007/s00703-010-0068-x.

Skamarock, W. C. and J. B. Klemp (2008), A time-split nonhydrostatic atmospheric model for weather research and forecasting applications, *J. Comp. Phys., 227,* 3465-3485.

Backup Slides

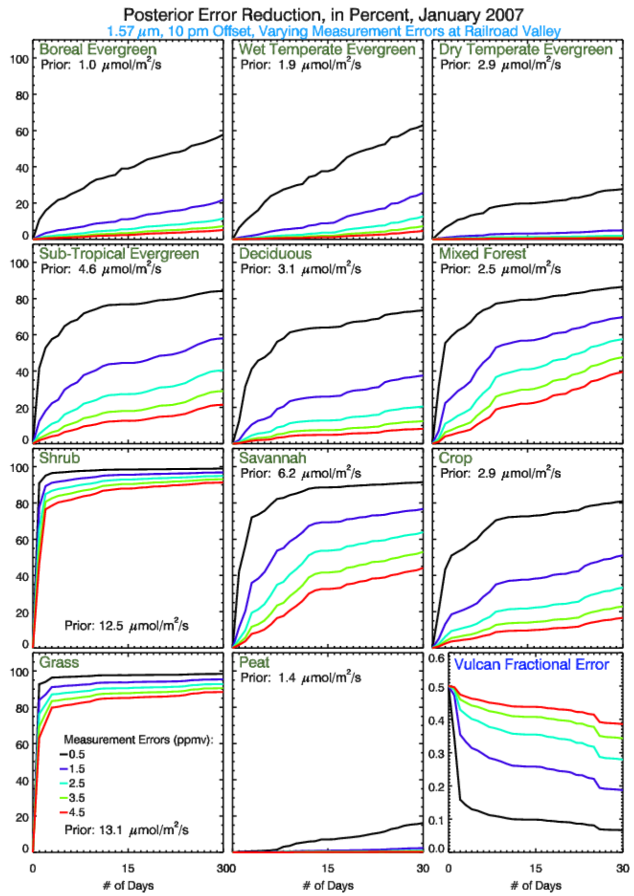

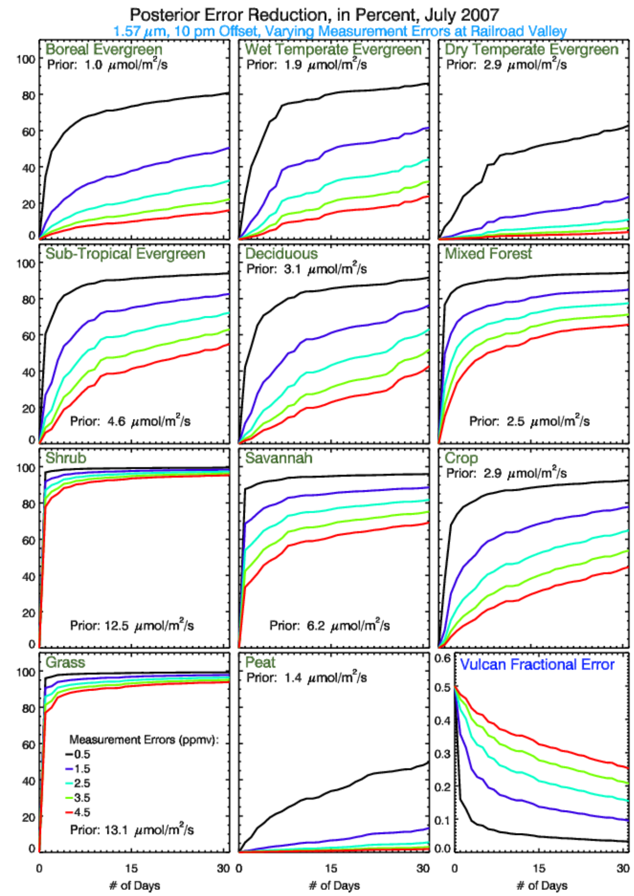

Backup Slides

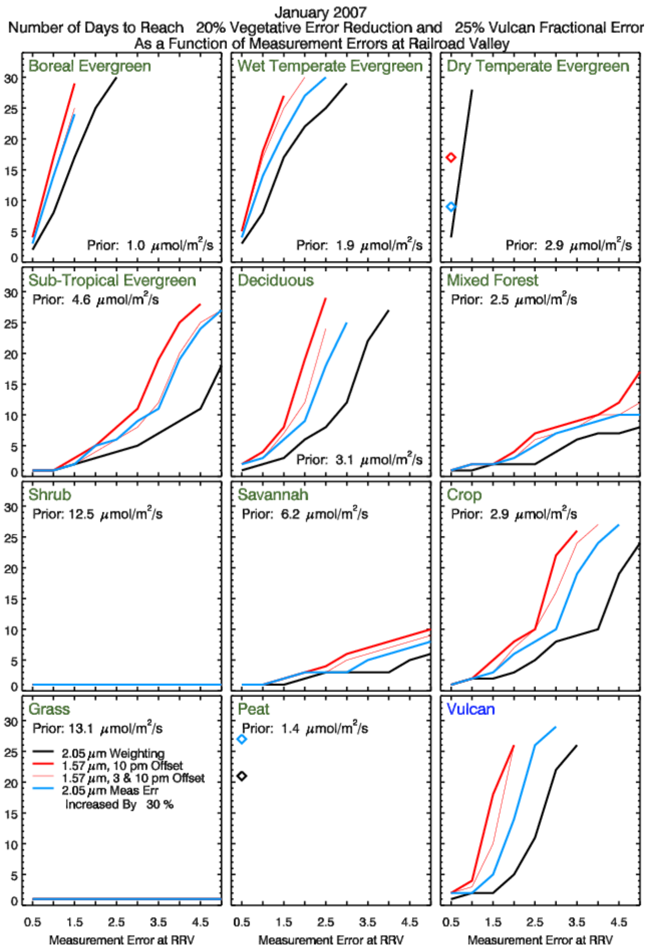

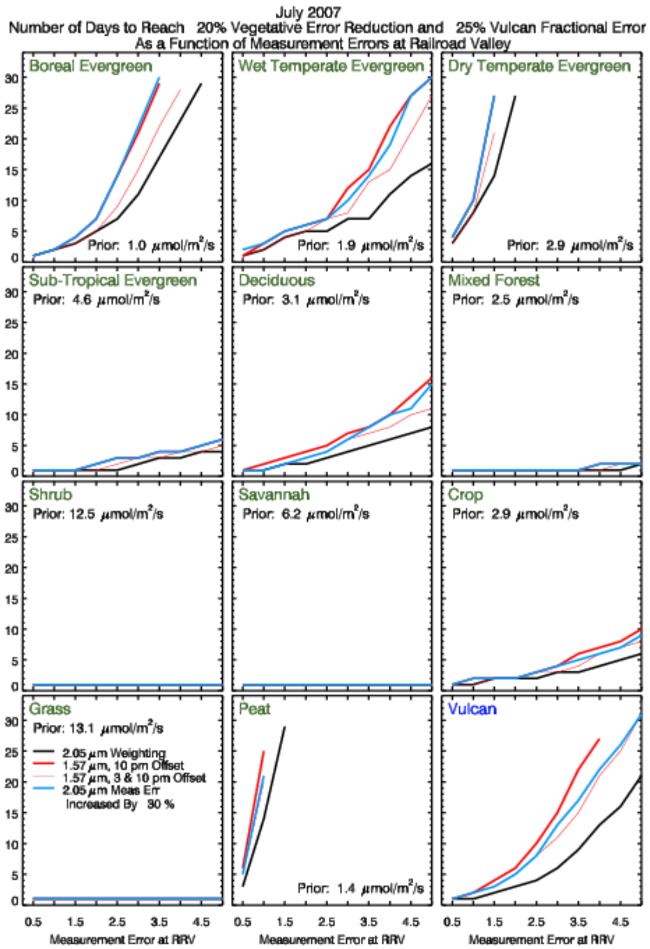

Atmospheric and Environmental Research